Experimental Investigation of the Effect of Transient Overvoltages on XLPE-insulated HVDC Cables

Experimental Investigation of the Effect of Transient Overvoltages on XLPE-insulated HVDC Cables

Bassel Diban, *Member, IEEE*, Giovanni Mazzanti, *Fellow, IEEE*, Laura Mazzocchetti, *Member, IEEE*, and Paolo Seri, *Member, IEEE*

***Abstract*— HVDC cables are subject to several types of impulses superimposed on the rated DC voltage during their service lifetime. Temporary Overvoltages (TOVs) and Superimposed Switching impulses (SSIs) are considered some of the most challenging due to the relatively long impulse duration. This paper aims at investigating experimentally the effect of TOVs and SSIs on XLPE insulation for extruded HVDC cables. 0.15-mm-thick DC-XLPE specimens, aged by applying TOVs and SSIs, are characterized using dielectric analyzer and Fourier Transform InfraRed spectroscopy (FTIR) to detect the aging effects on the insulation. Results show an increase in the imaginary part of permittivity, ε", accompanied with the appearance of additional dipolar polarization losses peaks. The amplitude and frequency of the aforementioned peaks vary with the amplitude and the number of applied TOVs and SSIs. An increase in electrical conductivity is also noticed with aging. FTIR results show absorbance peaks in the aged specimens likely due to the intramolecular bonds rupture accompanied with the formation of aging products. In summary, SSIs and TOVs cause a noticeable reduction of insulating properties in XLPE specimens. The higher the peak of the transient, the greater the aging effect.**

***Index Terms*— Accelerated aging, cable insulation, HVDC transmission, impulses, transient, spectroscopy.**

I. INTRODUCTION

HVDC cable systems have recently gained a great attention due to their application in linking renewable energy sources with load centers [1, 2]. HVDC cables are subject to several types of transient overvoltages during the normal operation as well as contingencies. Among those transients, Superimposed Switching Impulses (SSIs) and Temporary Overvoltages (TOVs) are part of the most challenging to the electrical power system. They are always superimposed on the – more or less – constant rated DC voltage of the transmission system [2]. The progressive increase in the rated voltage of HVDC cable systems leads to a greater amplitude of transients, which becomes more challenging. Therefore, studying the effect of such transients becomes important and crucial. In [3–5] the authors performed simulations using a life model-based procedure to investigate the effect of both SSIs and TOVs on the electrothermal life of HVDC cables. According to these simulations, the aging effect of TOVs and SSIs on the reliability of existing HVDC extruded cables in service is essentially negligible. However, the results of these simulations require an experimental confirmation for existing cables; moreover, they might not hold for the new generation of HVDC extruded cable insulations developed and designed to withstand higher electric fields [2, 6, 7]. Other studies investigate the effect of different types and frequencies of electrical transients on the aging process in insulating materials. In [8], M. Ghassemi found a reduction in the life of wires insulation when the transient slew rate is increased, highlighting the critical effect of fast transients on the degradation of insulating materials. In [9, 10], commutation voltage transients reduce both the life and the Voltage Endurance Coefficient (VEC) of wires insulation which in turn accelerates the aging process. In [11], F. Mauseth *et. al* investigated the effect of high frequency AC voltage, superimposed on the DC voltage, on the aging process in XLPE insulation and found that it causes a significant reduction in the breakdown voltage. However, no studies that reveal the effect of SSIs or TOVs on the HVDC cable insulations are found in the literature so far. This study aims at an experimental assessment of the effect of both TOVs and SSIs on the reliability and aging of XLPE insulating material. In this study, impulse trains of TOVs and SSIs are applied on flat XLPE samples, which are characterized later by:

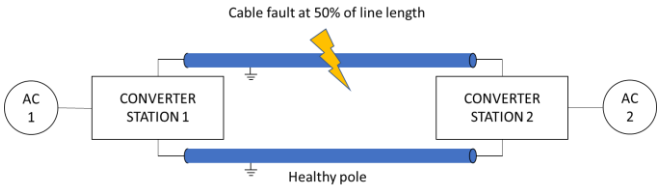

Fig. 1. Schematic of the faulted VSC HVDC transmission system giving rise to a TOV on the healthy pole of a symmetric monopolar HVDC link.

Bassel Diban, Giovanni Mazzanti and Paolo Seri are with the Department of Electrical, Electronic and Information Engineering (DEI), Alma Mater Studiorum–University of Bologna, 40136 Bologna, Italy (e-mail: bassel.diban2@unibo.it).

Laura Mazzocchetti is with the Department of Industrial Chemistry "Toso Montanari", Alma Mater Studiorum–University of Bologna, 40136 Bologna, Italy.

Color versions of one or more of the figures in this article are available online at http://ieeexplore.ieee.org

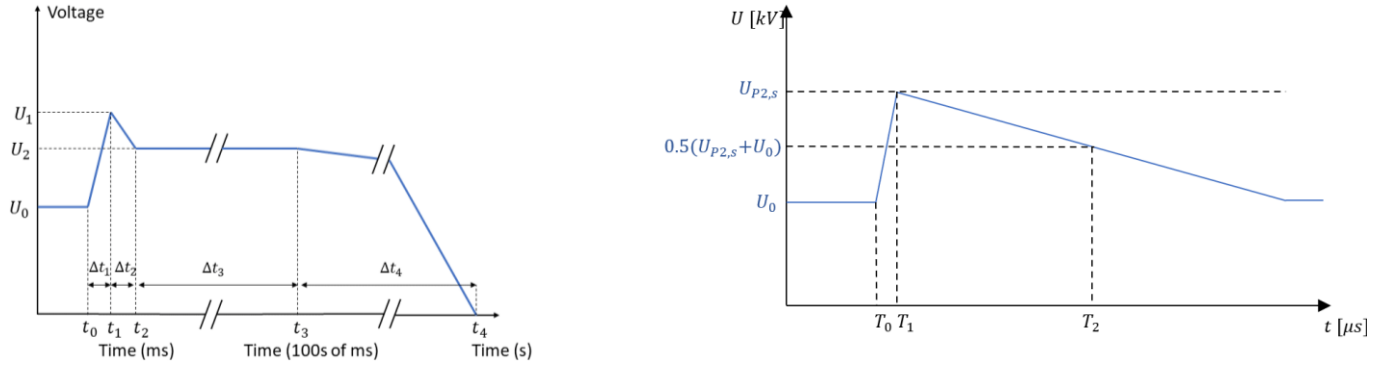

Fig. 2. Waveshapes of (a) Temporary Overvoltage TOV and (b) Superimposed Switching Impulse SSI of same polarity, both superimposed on the DC voltage according to [12–14], respectively.

- dielectric spectroscopy;
- DC current measurements;
- Fourier Transform InfraRed spectroscopy (FTIR).

The electric field levels – as well as the number of pulses for the TOVs – applied in these laboratory tests are significantly increased compared to those encountered in service conditions, to accelerate the possible aging effects of TOVs and SSIs, and enable their detection via dielectric spectroscopy, DC current measurements and FTIR. In this way, a more detailed analysis of the possible aging effects is carried out by varying the amplitude and the number of impulses in order to extrapolate the obtained results to possible scenarios of different operational cases in the power grid.

II. Experimental Methods

This section illustrates in detail the experimental aging setup, from impulses waveshape generation to spectroscopic measurements.

A. Waveshapes

TOVs occur on the healthy pole of an HVDC transmission system in both symmetric monopolar and rigid bipolar configurations when a pole-to-ground fault takes place on the other pole (Fig. 1). The post-fault voltage rises to reach the peak with a rise time in order of few ms, then it gets limited by the surge arresters of the HVDC converter station which maintain the plateau voltage for hundreds of ms until the cable is fully discharged withing few minutes [12]. Extensive simulations considering different fault types showed that pole-to-ground faults in the middle of the negative pole of a symmetric monopolar VSC HVDC cable system leads to the most severe (or "worst case") TOVs on the healthy pole i.e. a voltage up to 1.8 times the pre-fault DC voltage [3] (as shown in Table I), or even higher. The SSIs – which occurs mainly due to switching events – are defined according to IEC Standard 60060-1 [13]. The SSI has a rise time and a time to half-value on the tail of 250 and 2500 µs, respectively. The maximum peak value of the SSI of the same polarity superimposed to the DC voltage, $U_{P2,s,min}$, is calculated according to CIGRÉ Technical Brochure 496 [14] as follows:

TABLE I
WORST CASE TOV AND SSI WAVESHAPES CHARACTERISTICS

impulse type	symbol	parameter	value and unit
TOV (after [12])	U_a	Peak voltage	1.8 p.u.
	U_b	Plateau voltage	[1.5–1.6] p.u.
	Δt_1	Time to peak	[0.5–5] ms **2** ms
	Δt_2	Time of peak decay	[0.5–5] ms **2** ms
	Δt_3	Time of plateau	[100–**200**] ms
	Δt_4	Discharge time	[30–>600] s **45** s
	T_{TOV}	Duration of TOV	45.2 s
SSI (after [13,14])	$U_{P2,s}$	Peak voltage	2.2 p.u.
	T_1	Front duration	250 µs
	T_2	Time-to-half	2500 µs
	T_{SSI}	Duration of SSI	4.75 ms

TABLE II
TOTAL DURATION OF TOV AND SSI AGING PROCESS

impulse type	Time interval between consecutive impulses	Total duration	
		1000 impulses	2000 impulses
TOV	1 s	12.8 hours	25.7 hours
SSI	1 s	17 minutes	34 minutes

TABLE III
TOV AND SSI APPLIED VOLTAGES DURING THE AGING PROCESS

impulse type	E_0 (kV/mm)	voltage type	value (kV)
TOV	25	Peak (1.8 E_0)	6.75
		Plateau (1.5 E_0)	5.625
	50	Peak (1.8 E_0)	13.5
		Plateau (1.5 E_0)	11.25
SSI	25	Peak (2.2 E_0)	8.25
	50	Peak (2.2 E_0)	16.5

$$U_{P2,s,min} = 1.15\ U_T = 1.15 * 1.85\ U_0 = 2.13\ U_0 \quad (1)$$

where U_T is the voltage applied during the Type Test [14], while U_0 is the nominal DC voltage. As a conservative value, $2.13U_0$ is rounded to $2.2U_0$. Table I presents the waveshape characteristics of both TOVs and SSIs. The numbers in bold are chosen to carry out the experimental results in this work. This choice is so that the highest number of TOVs (maximum stress) is applied in a given time interval.

Two durations of the test (Table II) and two electric field levels (Table III) are selected in these tests to simulate different numbers and amplitudes of TOVs and SSIs.

For both TOVs and SSIs the number of impulses applied in the aging process are 1000 and 2000 at a frequency of 1 Hz – i.e. with a time interval of 1 s between each two consecutive impulses – as illustrated in Table II, which includes the total duration of TOV and SSI aging tests. It is worthwhile pointing out that – notwithstanding the pulses have the same 1 Hz frequency for both TOVs and SSIs – the total duration of TOVs aging process is much longer than that in the case of SSIs, as the duration of one single TOV (45.2 s) is much greater than that of one single SSI (4.75 ms), as shown in Table I. The frequency and number of surges applied in the aging tests are significantly greater than those encountered in service conditions; this holds especially for the TOVs, which are associated with pole faults. These values of frequency and number are chosen to accelerate the possible aging effects of TOVs and SSIs, thereby easing their detection after the tests.

The chosen values of the rated electric field E_0, i.e. the DC component of the field at rated voltage U_0 are (as shown in Table III):

- 25 kV/mm, which is a typical design electric field in the state-of-the-art HVDC cables [15].
- 50 kV/mm, which represents an upper limit of the electric field in the new generation of HVDC cables (e.g. 800 kV cables), and also serves to accelerate the aging effect of electric field on dielectric properties and the aging of XLPE insulating material [6].

Values of the peak and plateau voltages for TOVs, as well as the peak voltage of SSIs, are reported in Table III, for each chosen value of E_0.

B. Experimental Setup

This experiment consists of two main stages i.e. aging and measurements. The aging procedure begins with a custom-made low-voltage 13-bit digital-to-analog converter which is used as a low voltage signal generator (for either TOVs or SSIs). It is programmed to generate and replicate the impulse waveshapes shown in Fig. 2 for a given number of impulses. Then, impulses are amplified to the voltages shown in Table III using a Trek 30/20 high voltage amplifier. High voltage impulses are repetitively applied on XLPE specimens clamped between two circular flat electrodes (with radius of 20 mm) at room temperature [16].

After the aging tests, dielectric spectroscopy and Fourier Transform InfraRed spectroscopy (FTIR) measurements are performed on aged and unaged specimens to assess the effect of aging on the dielectric properties and polymeric structure of XLPE. Details on these measurements are given in the next chapters.

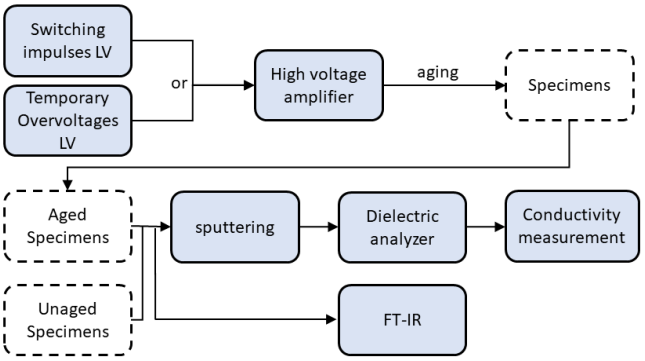

Fig. 3. Block diagram that shows the aging and measuring processes.

C. Specimens

Specimens used in this experiment are flat samples (peelings) of DC-XLPE which are initially used in the framework of the European project ARTEMIS. The thickness of each sample is measured accurately using an electronic micrometer. The measured thickness of specimens falls in the range of [0.147–0.152] mm. Five specimens are tested for each aging case to allow a statistical processing of results. The chosen number of specimens is a compromise between the test duration (especially for TOVs, which can require up to >24 hours per specimen) and the ability to describe an average trend of the population. As a consequence of the relatively small sample and population size, Student's t-distribution with 5 degrees of freedom and a 95% confidence interval, is used to estimate the mean value of the real and imaginary permittivity, as shown in Equation (2):

$$\bar{m} - 2.571\ s/\sqrt{n} \leq \mu \leq \bar{m} + 2.571\ s/\sqrt{n} \quad (2)$$

where $\bar{m}$ is the mean value of the sample, s is the standard deviation, n is the number of tested specimens and μ is the mean value of the population.

D. Dielectric Spectroscopy

Golden electrodes were deposited on both sides of specimens by cold sputtering under 0.15 mbar pressure of Argon during 300 seconds. This is necessary to ensure an ideal contact interface during dielectric spectroscopy. A Novocontrol Alpha-A dielectric Analyzer is used to measure the complex permittivity of aged and unaged XLPE specimens. Dielectric spectroscopy was carried out under a voltage of 3 (V_{rms}), frequency range [10^{-2} –10^{6}] Hz, and a temperature of 25 (°C). The complex permittivity ε consists of real and imaginary parts, as illustrated in Equation (3); the real part ε' represents the dielectric constant of the material. The imaginary permittivity ε'' consists of two terms as illustrated in Equation (4), the first one γ/ω considers conduction process in the insulation, while the other term ε_h'' represents the contribution of dipolar losses [17].

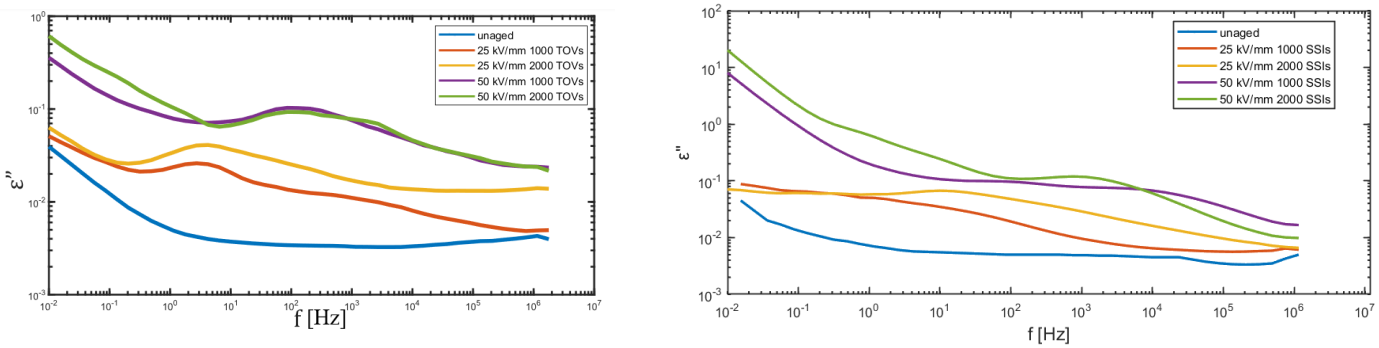

Fig. 4. The mean value of the imaginary permittivity vs frequency in a log-log scale for both unaged and aged specimens with two different values of number (1000 and 2000) and amplitude (E_0=25 kV/mm and 50 kV/mm) of (a) Temporary Overvoltages TOVs (after[17]) and (b) Superimposed Switching Impulses SSIs.

$$\varepsilon = \varepsilon' - j\varepsilon'' \tag{3}$$

$$\varepsilon'' = \gamma/\omega + \varepsilon_h'' \tag{4}$$

where γ is electrical conductivity, ω is the angular frequency. It is worth noting that the conduction term dominates the imaginary permittivity as ω tends to 0; then, the logarithmic plot of ε'' over the applied frequency $f = \omega/2\pi$ eventually becomes a line with slope -1, below a certain frequency depending on the value of γ. Generally speaking, the higher the conductivity, the higher the frequency at which this phenomenon starts being noticeable.

E. DC Conductivity measurement:

DC conductivity measurements were carried out to find out the effect of the aging of XLPE specimens by SSIs impulses on the DC electrical conductivity. The setup consists of an insulated cell in which three electrodes are connected to measure the volume electrical conductivity as follows: the upper electrode is connected to the DC power supply (Fug HCN 35-35000) which is kept at 3 kV during the experiment to provide an electric field = 20 kV/mm inside the 0.15-mm thick specimen.

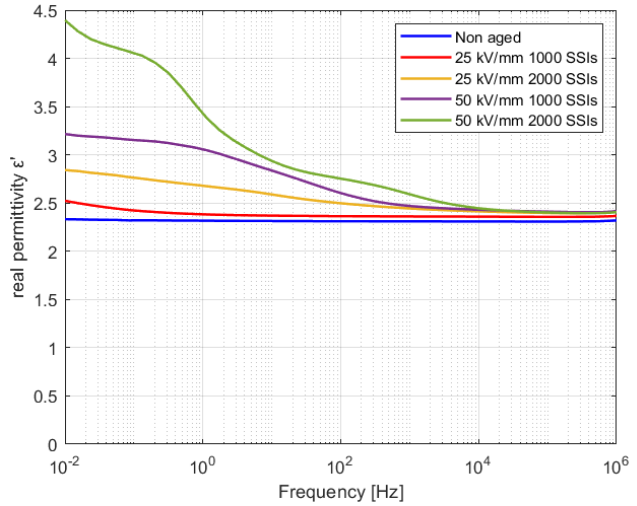

Fig. 5. The mean value of the real permittivity vs frequency in a semi-log scale for both unaged and aged specimens with two different values of number (1000 and 2000) and amplitude (E_0=25 kV/mm and 50 kV/mm) of Superimposed Switching Impulses SSIs.

While the lower electrode is connected to the KEYSIGHT B2981A Femto/Picoammeter, the guard ring is connected to earth to remove stray currents and ensure that the measured current is only the conduction current flowing in the bulk of the dielectric specimen.

F. FTIR

Fourier Transform InfraRed spectroscopy FTIR is used to detect the molecular composition of XLPE specimens. FTIR can detect the formation of new functional groups and characterizing bonding information using the transmittance (or the absorbance) in a certain frequency range of the wavelength commonly indicated by its reciprocal, which is the wavenumber (cm^{-1}). In this study, a Bruker ALPHA FTIR Spectrometer equipped with Attenuated Total Reflectance (ATR) with diamond crystal accessory allowing to measure solid specimens' chemistry is used to characterize the aged specimens as well as the unaged ones to compare them and detect any variation of the XLPE material or formation of new aging bonds. The ATR tool allows for direct spectra recording on solid samples without specific preparation, thus being more representative of the actual specimen chemistry.

III. Results

A. Dielectric Spectroscopy

Fig. 4 presents the mean values of the Student's t-distribution for unaged specimens as well as specimens aged by TOVs (Fig. 4(a)) or SSIs (Fig. 4(b)) according to Tables II, III. Confidence bounds are not shown here for the sake of both brevity and comparison, hence, more details can be found in [16, 17]. It can be seen that the aging process by either TOVs or SSIs is characterized by a noticeable increase of the imaginary part of permittivity, ε", accompanied with the appearance of peaks at certain frequency bands.

This effect is particularly evident as the electric field E_0 is increased from 25 kV/mm to 50 kV/mm: the greater the applied electric field, the greater the increase of imaginary permittivity over the whole studied frequency range. This tendency is particularly clear for the TOVs, but it holds also for the SSIs, suggesting a general increase of dielectric losses due to electrical aging caused by these transient voltage waveforms at

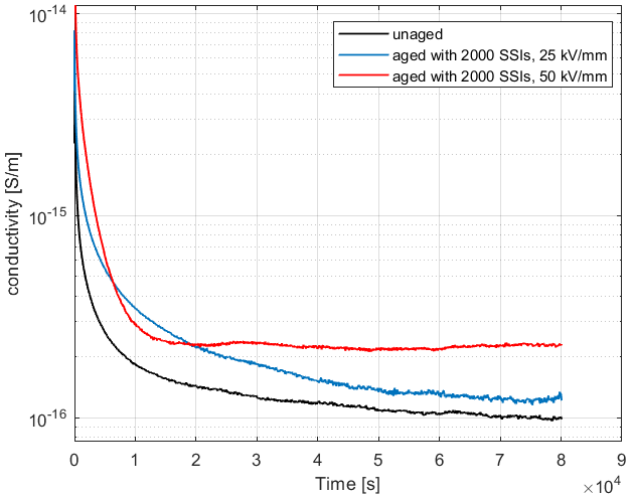

Fig. 6. DC current measurements on a specimen aged by 2000 SSIs for E_0=25 kV/mm and E_0=50 kV/mm at 25 °C and electric field E =20 kV/mm.

high fields. This might set a challenge especially to the new generation of HVDC extruded insulation, as discussed below.

The effect of the number of applied impulses is similar, but not so clear as for the electric field; indeed, the increment of ε" with the number of impulses is more evident in the medium and high frequency range at E_0=25 kV/mm, and in the low frequency range at E_0=50 kV/mm.

Both aging by TOVs and SSIs leads to a peak of ε" in the frequency range [1–10^2] Hz when E_0=25 kV/mm, while the peak loss falls in a higher frequency range, [10^2–10^4] Hz, for E_0=50 kV/mm. This suggests the formation of polar molecules due to the aging process, which in turn are increasing the dipolar losses in the range [1–10^4] Hz. Fig. 4 also shows a significant increment for frequencies below 1 Hz.

Moreover, Fig. 4 indicates that, especially at 50 kV/mm, the aging effect on conductivity in case of SSIs is greater than that in case of TOVs, although the polarization peaks in both TOVs and SSIs have approximately the same order of magnitude. This result might indicate an increase of the electrical conductivity γ of aged insulation, compared to the unaged one. Such increase should result in higher values of the term γ/ω in Equation (4), and an increase of the imaginary part of permittivity with a linear trend with slope of -1, as ω tends to 0 in bi-logarithmic scale, which is confirmed by conductivity measurement results.

Fig. 5 illustrates the real permittivity variation after the aging of specimens using SSIs. It is clearly seen that only a slight increase in the real permittivity can be noticed for frequencies greater than 10^4 due to aging process. However, for lower frequencies i.e. [10^{-2}–10^4], the real permittivity increases as the frequency tends to 0; such increase is mild at E_0=25 kV/mm, more significant at E_0=50 kV/mm, especially as the number of impulses is increased from 1000 to 2000. Also the increment slope is greater for higher number and/or amplitude of the SSIs impulses.

B. Conductivity

To verify the conductivity rise due to SSIs, DC conductivity measurements were performed according to IEC 62631 standards [18] on an unaged specimen and a specimen aged by 2000 SSIs with an electric field E_0 of 25 kV/mm and 50 kV/mm. The temperature during the experiment was fixed at 25 °C and a constant voltage of 3 kV was applied on the specimens such that the electric field is equal to 20 kV/mm. As it can be seen in Fig. 6, the electrical conductivity is increased after the aging process due to SSIs: at 25 kV/mm it is increased by ≈ 25 %, but it is particularly doubled at 50 kV/mm. As the electrical conductivity is one of the most critical properties used to assess the overall quality and performance of HVDC cable insulation, these measurements suggest that for the new generation of HVDC extruded cables a high number of switching impulses might set a challenge to the useful service life of the cable.

C. FTIR

Fig. 7 shows the results of FTIR spectroscopy measurements performed for unaged and aged specimens subjected to either TOVs (Fig. 7(a)) or SSIs (Fig. 7(b)). Those Figures plot the transmittance of the IR waves in a certain range of the wave length represented here by the wavenumber [400 – 4000] cm^{-1}

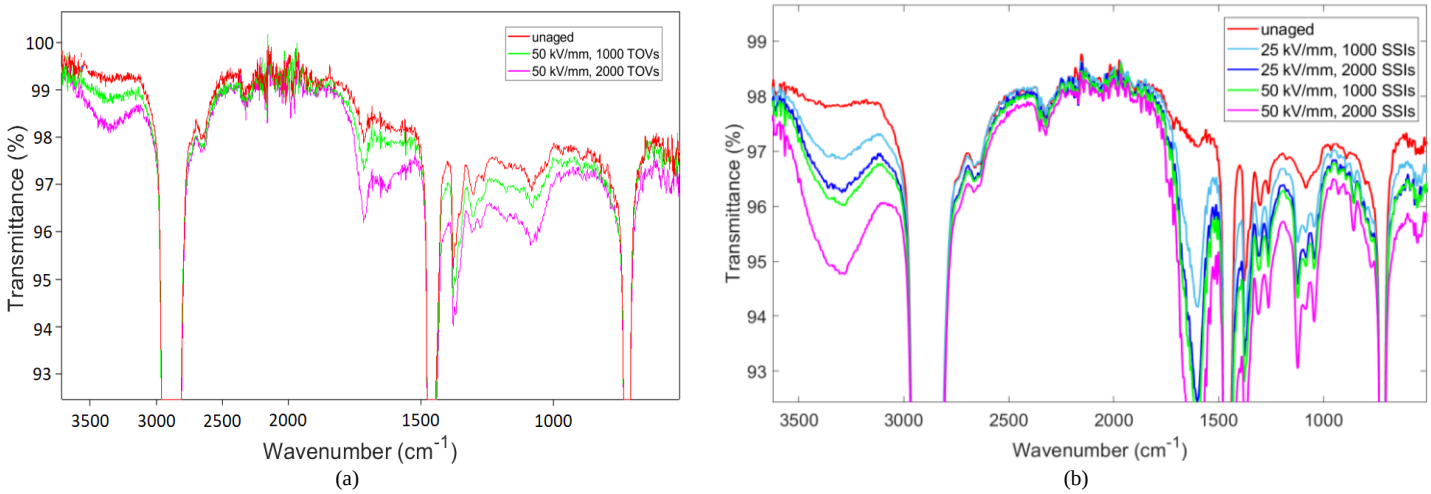

Fig. 7. The mean value of the transmittance of unaged samples and samples aged by (a) Temporary Overvoltages TOVs and (b) Superimposed Switching Impulses SSIs, measured by Fourier Transform Infrared Spectroscopy FTIR in the range of transmittance [93–100]%.

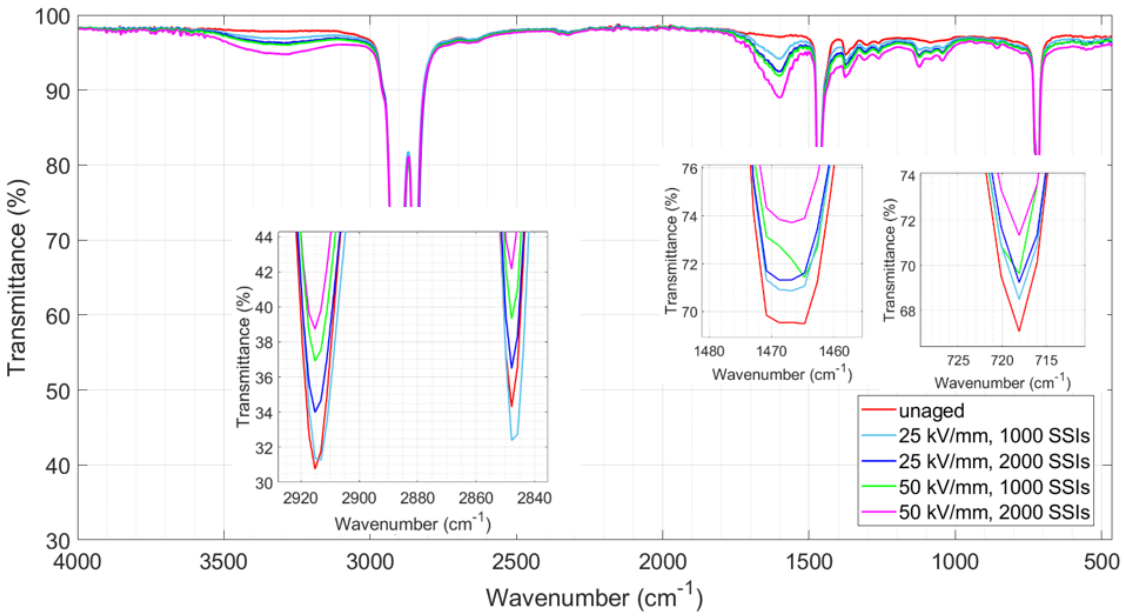

Fig. 8. The mean value of the transmittance of unaged samples and samples aged by Superimposed Switching Impulses SSIs, measured by Fourier Transform Infrared Spectroscopy FTIR highlighting the variation of transmittance drops of XLPE in 3 zoom-in insets.

. Polyethylene (PE) is characterized by 3 strong absorption peaks or conversely transmittance drops, (they are referred to as "absorption peaks" hereafter) [19] attributed to the aliphatic chain:

- 2870 cm^{-1} corresponds to the stretching vibration of the C–H bond of methylene which includes two peaks: 2915 cm^{-1} and 2850 cm^{-1} for CH_2 asymmetric and symmetric stretching, respectively;
- 1460 cm^{-1} corresponds to the bending vibration of the methylene C–H bond;
- 720 cm^{-1} corresponds to the rocking vibration of the methylene C–H bond.

Additionally, other smaller peaks can be observed at the wave numbers 1377, 1306 and 1176 which corresponds to CH_3 symmetric deformation, twisting deformation and wagging deformation respectively (see strong peaks in the insets of Fig. 8). While the aforementioned characteristics are related to the unaged and aged XLPE samples, both TOVs and SSIs aging processes cause a considerable variation in the transmittance at certain wavenumber bands as follows:

1) A decrease of the IR transmittance (increase of absorption) at 4 wavenumber bands is observed by comparing the unaged mean curve with the mean curve of samples aged by either TOVs or SSIs:

- [740–1450], the absorption peak of C=C bond increased with aging field's amplitude and time. The latter change might be related to oxidative cracking reaction which leads to the formation of aging products belonging to the vinylene group [20, 21]. Additionally, the peaks in this band might be also caused by the vibrations of –C–O–C– ether bonds [22, 23].
- [1500–1750] cm^{-1}: the absorption peak in this regions is ascribed to the possible formation of C=O and C=C bonds. Free radicals caused by the C–C bond rupture might be combined with oxygen to form carbonyl groups C=O, carboxylic acid RC(=O) OH, ketones RC(=O) R' or ester RC(=O) OR' [23].
- [3000–3500] cm^{-1}, the absorption peak at this wavenumber is typical of the O-H stretching that might belong either to the formation of carboxylic acid groups R–COOH and hydroxyl groups R–OH [24] both resulting from oxidative ageing processes;

2) An increase of the IR transmittance (decrease of absorption) of characteristic XLPE peaks (720, 1460, 2850 to 2915 cm^{-1}) after the aging process. This could be a result of molecular chain scissions in XLPE by which the above-mentioned aging byproducts are formed.

Fig. 8 presents the full scale plot of the FTIR spectroscopy for unaged samples and samples aged with SSIs highlighting three clearly increasing absorption peaks.

As a comparison between the FTIR results of samples aged by TOVs and SSIs, it can be seen in Fig. 7 that the transmittance of IR is reduced in SSIs approximately twice that in case of TOVs, for the same E_0 and the number of impulses. This might be the cause of the different levels of conductivity increase noticed in the previous section. Consequently, according to the results of these measurements, the effect of the applied SSIs on the aging of the tested XLPE insulation specimens seems to be more severe than that of the applied TOVs, although the duration of an SSI is much shorter than that of a TOV. On the other hand, the insulating material aged with SSIs is subjected

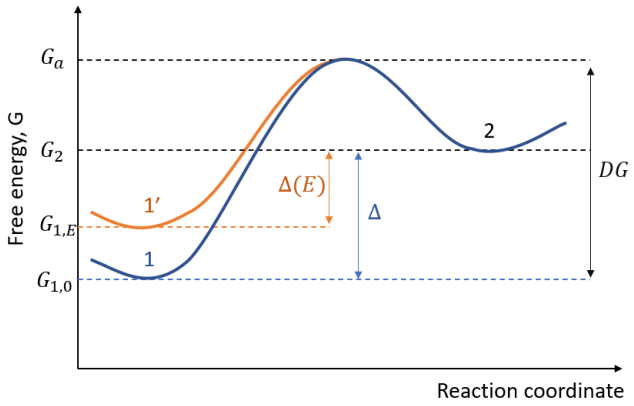

Fig. 9. Free energy diagram in the presence of electric field (after [27]).

to a peak electric field 20% greater than that in the case of TOV aging. This result highlights the strong impact of a small increase in the applied field on aging. The long plateau duration of TOVs seems to have no noteworthy effect on the aging of XLPE, compared to the effects of a higher field, despite a shorter duration of the stress.

IV. Discussion

Many proposals of the electrical aging mechanisms in polymeric insulations can be found in the literature, as shown e.g. in [25–33]. In [25], experimental results suggest that most physical and chemical aging processes occurs in free volume and/or sub-microcavities [28] inside the insulation or at its interfaces. Two mechanisms of electrical aging can be distinguished according to the amplitude of the electric field distributed inside the insulation:

- low (operational) electric fields: electrons in sub-excitation state are not expected to cause a chemical damage but a morphological change in the insulating material, where the electron moves as a polaron or by trapping/detrapping with energy that is sufficient to break only intermolecular bonds [25].
- high electric field: when a high electric field is applied on the insulation, hot electrons in microcavities in the bulk probably gain sufficient energy to cause intramolecular bonds rupture (i.e. C-H or C-C bonds in the molecular structure) in the insulation surface near the voids [25,28], which in turn allows oxidation reactions and the formation of aging products. Starting from the thermodynamic concept of a free-energy barrier for degradation that can be lowered by an applied electric field [26], Dissado, Mazzanti, and Montanari in [27] and Crine in [28] introduced an electronic aging model in the presence of space charges due to the reduction of the free-energy barrier from Δ to $\Delta(E) < \Delta$ as illustrated in Fig. 9. The reduction in the free-energy barrier could be translated into fatigue in the Van der Waals bonds leading to free-volume rearrangement and/or expansion [28]. The latter likely induces partially reversible / partially permanent deformation of the insulation leading at the end to sub-microcavities formation and expansion [27,28]. Ionization in the gaseous molecules in free volume and/or sub-microcavities might contribute to the aging process, since it triggers and sustains localized electrical discharges within the insulation which increase the chemical damage inside the dielectric [25].

In this respect, it is worth pointing out that PD measurements were not considered as one of the parameters to understand the aging process under exam since - as the other measurements suggest - the aging process during the measurements has not reached a strong degradation of the dielectric yet, but it seems to be still at an early stage. At such stage, free volume expansion is more likely to have taken place rather than the formation of sub-microcavities large enough to sustain PD activity. Furthermore, PD measurements are unable to give an accurate answer to the question whether the aging process is still involving only free volume expansion or it has progressed to micro/sub microcavities formation and/or expansion. Not to mention that PD measuring techniques currently available are used for PD detection in relatively large defects. However, PD measurements on a large, intentionally made defect model is an interesting topic for a future work to detect the effect of insulation aging due to TOVs or SSIs on PD inception voltage (PDIV).

Other aging phenomena attributed to relatively long impulse duration i.e. TOV might be fast charge packets [34]. Fast packets are clusters of electrons or ions with a high mobility value. Such packets could cause hetero charge layer in inside the insulation which is expected to accelerate and enhance the above-mentioned space charge electronic aging. This phenomena is not likely to occur in SSI because its duration is much shorter [4].

Another possible mechanism could be involving electromechanical stresses [35] able to cause local and global plastic strain and craze formation, from which energetic phenomena (such as partial discharges) can start incepting, eventually bringing the insulation to failure.

V. Conclusion

This study investigated how overvoltage transients (both Superimposed Switching Impulses (SSIs) and Temporary Overvoltages (TOVs)) can accelerate aging phenomena in XLPE insulation. Results show a noticeable incremental reduction of insulating properties in specimens aged under those temporary overstresses, especially at higher fields. Dielectric spectroscopy shows an increase of both conductivity and dipolar losses. Indeed, SSIs clearly enhance losses at low frequencies, while the effect of TOVs is more evident at higher frequencies, for the same rated field and number of impulses. This was confirmed by conductivity measurements and dielectric spectroscopy are consistent with Fourier Transform InfraRed spectroscopy FTIR results, which show a noticeable rupture in the covalent C–C and/or C–H bonds in the XLPE molecular structure accompanied with the formation of new aging products. As the electrical conductivity is one of the most critical properties in dielectrics for HVDC applications, these results suggest that a high number of switching impulses might set a challenge to the reliability of

the new generation of HVDC extruded cables, which might be targeted by premature aging due to the combination of high electric fields a number of transient events.

Of course, other measurements can be performed to confirm the results obtained by performing conductivity measurements, dielectric spectroscopy and FTIR measurements. For example, space charge measurements can give an indication on the ability of the XLPE specimens to store charges in addition to any possible variation in the trap depth due to the material aging. For this reason, space charge measurements are ongoing and the relevant results are planned to be presented in the early future.

REFERENCES

[1] G. Mazzanti and M. Marzinotto, *Extruded Cables for High Voltage Direct Current Transmission: Advance in Research and Development*, Power Engineering Series, Wiley-IEEE Press, 2013.
[2] G. Mazzanti, “Issues and challenges for HVDC extruded cable systems”, Energies (MDPI), vol. 14, no. 15, pp. 1-34, 2021.
[3] G. Mazzanti and B. Diban, "The Effects of Transient Overvoltages on the Reliability of HVDC Extruded Cables. Part 1: long temporary overvoltages," IEEE Trans. Power Deliv., vol. 36, no. 6, pp. 3784-3794, Dec. 2021.
[4] G. Mazzanti and B. Diban, "The Effects of Transient Overvoltages on the Reliability of HVDC Extruded Cables. Part 2: Superimposed Switching Impulses," IEEE Trans. Power Deliv. vol. 36, no. 6, pp. 3795-3804, Dec. 2021.
[5] G. Mazzanti, "Improved Evaluation of the Life Lost by HVDC Extruded Cables due to Long TOVs," in IEEE Trans. Power Deliv., vol. 37, no. 3, pp. 1906-1915, June 2022.
[6] M. Jeroense, P. Bergelin, T. Quist, A. Abbasi, H. Rapp, and L. Wang, “Fully qualified 640 kV underground extruded DC cable system,” paper B1-309, 2018 CIGRE Session, 2018.
[7] M. Albertini, S. Franchi Bononi, S. Giannini, G. Mazzanti, N. Guerrini, “Testing challenges in the development of innovative extruded insulation for HVDC cables”, IEEE Electr. Insul. Mag., Vol. 37, No. 6, pp. 21-32, Nov./Dec. 2021.
[8] M. Ghassemi, "Accelerated insulation aging due to fast, repetitive voltages: A review identifying challenges and future research needs," in IEEE Trans. Dielectr. Electr. Insul., vol. 26, no. 5, pp. 1558-1568, Oct. 2019.
[9] G. C. Montanari, P. Morshuis, P. Seri, R. Ghosh, . Ageing and reliability of electrical insulation: the risk of hybrid AC/DC grids. *High Voltage*, vol.5, no.5, pp.620-627, 2020.
[10] G. C. Montanari and P. Seri, "The effect of inverter characteristics on partial discharge and life behavior of wire insulation," in IEEE Electr. Insul., vol. 34, no. 2, pp. 32-39, Mag., 2018.
[11] F., Mauseth, et al. "Influence of DC Stress Superimposed with High Frequency AC on Water Tree Growth in XLPE Insulation." *Proceedings of the 23’rd Nordic Insulation Symposium*, Trondheim, Norway, June 9 - 12, 2013.
[12] M. Saltzer *et al.* “Overvoltages experienced by DC cables within an HVDC transmission system in a rigid bipolar configuration,” JICABLE’15, paper C5.1, Versailles (France), June 23-27 2019.
[13] IEC 60060-1, High-voltage test techniques. Part 1: General definitions and test requirements, Ed. 3, 2010.
[14] Recommendations for Testing DC Extruded Cable Systems for Power Transmission at a Rated Voltage up to 500kV, CIGRÉ Technical Brochure 496, 2012.
[15] A. Bareggi *et al.* “Current and future applications of HPTE insulated cables systems,” Paper B1-307, CIGRÉ Science & Engineering, no.13, pp. 34-44, Feb. 2019.
[16] G. Mazzanti, P. Seri and B. Diban, "Preliminary Experimental Investigation of the Effect of Superimposed Switching Impulses on XLPE-insulated HVDC Cables," *2021 IEEE Electr. Insul. Conf. (EIC)*, 2021, pp. 169-172.
[17] G. Mazzanti, P. Seri, B. Diban and S. Stagni, "Preliminary Experimental Investigation of the Effect of Long Temporary Overvoltages on the Reliability of HVDC Extruded Cables," 2020 *IEEE 3rd Int. Conf. Dielectr. (ICD)*, 2020, pp. 49-52.
[18] IEC 62631-3-1, Dielectric and resistive properties of solid insulating materials - Part 3-1: Determination of resistive properties (DC methods) - Volume resistance and volume resistivity - General method, Ed. 1, 2016.
[19] J. V. Gulmine, et al. "Polyethylene characterization by FTIR," Polymer testing, vol. 21, no. 5, pp. 557-563, 2002.
[20] B. Ouyang, H. Li, X. Zhang, S. Wang and J. Li, “The role of microstructure changes on space charge distribution of XLPE during thermooxidative aging,” IEEE Trans. Dielectr. Electr. Insul., vol. 24, no. 6, pp. 3849-3859, 2017.
[21] Y. Liu, H. Liu, L. Yu, Y. Li and L. Gao, “Effect of thermal stress on the space charge distribution of 160 kV HVDC cable insulation material,” IEEE Trans. Dielectr. Electr. Insul., vol. 24, no. 3, pp. 1355-1364, Jun. 2017.
[22] A. M. Nobrega, M. L. B. Martinez and A. A. A. de Queiroz, “Investigation and analysis of electrical aging of XLPE insulation for medium voltage covered conductors manufactured in Brazil,” IEEE Trans. Dielectr. Electr. Insul., vol. 20, no. 2, pp. 628-640, Apr. 2013.
[23] X. Chi *et al.* "Thermal-oxidative aging effects on the dielectric properties of nuclear cable insulation," Materials, vol. 13, no. 10, pp. 2215, 2020.
[24] Y. Kemari, A. Mekhaldi, G. Teyssèdre and M. Teguar, "Correlations between structural changes and dielectric behavior of thermally aged XLPE," IEEE Trans. Dielectr. Electr. Insul., vol. 26, no. 6, pp. 1859-1866, 2019.
[25] L. Sanche, "Nanoscopic aspects of electronic aging in dielectrics," IEEE Trans. Dielectr. Electric. Insul., vol. 4, no. 5, pp. 507-543, Oct. 1997.
[26] G.C. Montanari, G. Mazzanti, "From thermodynamic to phenomenological multistress models for insulating materials without or with evidence of threshold", J. Phys. D: App. Phys., Vol.27, pp.1691-1702, 1994.
[27] L. A. Dissado, G. Mazzanti and G. C. Montanari, "The role of trapped space charges in the electrical aging of insulating materials," IEEE Trans. Dielectr. Electr. Insul., vol. 4, no. 5, pp. 496-506, Oct. 1997.
[28] J. P.. Crine, "A molecular model to evaluate the impact of aging on space charges in polymer dielectrics," IEEE Trans. Dielectr. Electr. Insul., vol. 4, no. 5, pp. 487-495, Oct. 1997.
[29] G. Jiang, J. Kuang, S. Boggs, “Critical parameters for electrical tree formation in XLPE”, IEEE Trans. Power. Del., Vol. 13, pp. 292 - 296, 1998.
[30] T.J. Lewis, “Ageing - A perspective”, IEEE Electr. Insul. Mag., Vol. 17, No. 4, pp. 6-16, 2001.
[31] T.J. Lewis, “Polyethylene under electric stress”, IEEE Trans. Dielectr. Electr. Insul, Vol. 9, pp. 717-729, 2002.
[32] G. Teyssedre, C. Laurent, “Charge transport modeling in insulating polymers: from molecular to macroscopic scale”, IEEE Trans. Dielectr. Electr. Insul., Vol. 12, No. 5, pp. 857-875, Oct. 2005.
[33] C. Laurent, “Charge dynamics in polymeric materials and its relation to electrical aging”, *2012 IEEE Conf. Electr. Insul. Dielectr. Phenom. (CEIDP)*, 2012, pp. 1-20, Montreal (Canada).
[34] G.C. Montanari, "Bringing an insulation to failure: the role of space charge", IEEE Trans. Dielectr. Electr. Insul., vol. 18, pp.339–364, 2011.
[35] G. C. Montanari, P. Seri and L. A. Dissado, "Aging mechanisms of polymeric materials under DC electrical stress: A new approach and similarities to mechanical aging," IEEE Trans. Dielectr. Electr. Insul., vol. 26, no. 2, pp. 634-641, April 2019.

Bassel Diban (Member, IEEE) received the bachelor’s degree in electrical power engineering from Damascus University, Damascus, Syria (2014), then he joined the Syrian TSO for two years, and later received the master’s degree and the Ph.D. in electrical energy engineering from the University of Bologna, Bologna, Italy (2019, 2023), where he is currently working as a postdoctoral research fellow. His research interests are life modeling, reliability, diagnostics of HV insulation, and HVDC cable systems. Mr. Diban is a member of the IEEE DEIS Technical Committee (TC) on “High Voltage Direct-Current (HVDC) cable systems”.

Giovanni Mazzanti (Fellow, IEEE) is currently an Associate Professor of HV Engineering, Electrical Technologies and Power Quality at the University of Bologna, Bologna, Italy. He is Consultant to TERNA (the Italian TSO), Rome, Italy. His research interests are reliability and diagnostics of HV insulation, power quality, renewables, and human exposure to EMF. He has authored or coauthored more than 300 published papers, and book *Extruded Cables for HVDC Transmission: Advances in Research and Development*, (Wiley-IEEE Press, 2013).

Mr. Mazzanti is the Chair of the IEEE DEIS TC on “HVDC cable systems”, and member of IEEE PES and DEIS, CIGRÉ, CIGRÉ Joint Working Group B4/B1/C4.73, IEC TC 20/WG 16, EU IWG on HVDC Set Plan.

Paolo Seri (Member, IEEE) was born in Macerata, Italy, in June 4, 1986. He received the master’s degree in energy engineering and the Ph.D. degree in electrical engineering from the University of Bologna, Bologna, Italy, in 2012 and 2016, respectively.

In 2017, he was with the Laboratory of Innovative Materials for Electrical Systems (LIMES), University of Bologna, as a Research Fellow, where he is currently working on the topics of high voltage direct-current (HVDC) cables design, partial discharge detection and modeling, and characterization of dielectric materials. He is also a Researcher with the Department of Electrical, Electronic and Information Engineering (DEI), University of Bologna.